Effect of Al₂O₃ and SiC Nano Reinforcements on Microstructure, Mechanical and Wear Properties of Surface Nanocomposites Fabricated by Friction Stir Processing

Naresh PARUMANDLA [1, ∗]**, Kumar ADEPU** [2]

[1] *Mechanical Engineering Department, Madanapalle Institute of Technology & Science, Andhra Pradesh -517325, India*
[2] *Mechanical Engineering Department, National Institute of Technology Warangal, Telangana -506004, India*

In this study, friction stir processing has been applied to fabricate Al/Al₂O₃ and Al/SiC surface nanocomposites. Nano sized Al₂O₃, and SiC particles were used as a reinforcement whereas 6061-T6 aluminum alloy was selected as matrix material. The experiments were conducted at constant process parameters (1150 rpm and 15 mm/min) with changing volume percentage (2, 4 and 6) of nano reinforcements. The approach compared the effect of nano reinforcement on microstructural, mechanical, microhardness and wear properties of surface nanocomposites. Microstructure examinations revealed that Al₂O₃ and SiC nano particles were distributed into the processed region mainly in the form of clusters. Also, with increasing volume percentage of nano reinforcement increasing the defect formation. Vickers microhardness and tensile tests were conducted to study the mechanical properties of the surface nanocomposites. Superior microhardness properties were obtained along the stir zone. The addition of ceramic particle into the matrix material leads to increase in microhardness but simultaneously decreases yielding strength with an increase of wear resistance. The average coefficient of friction of Al/SiC composites were reduced than Al/Al₂O₃ composites. The effect of nano reinforcements on wear resistance was increased with increasing volume percentage of nano particles into the matrix material.
Keywords: surface nanocomposites, friction stir processing, microstructure, microhardness, wear characterization.

1. INTRODUCTION

In manufacturing industries, the use of high strength light weight material was increased because of their productivity efficiency in several applications. Aluminum alloys have best suitable properties like strength to weight ratio, but low wear resistance restricts its applications in manufacturing industries. Aluminum metal matrix composites (AMMCs) are the best replacement of monolithic materials [1, 2]. However, adding brittle ceramic reinforcements into the composites resists some of their applications [3], and dispersion of reinforcement particles in the composite region is challenging task while preparation of surface metal matrix composites (SMMCs) [4]. The distribution of ceramic particles on the metallic substrate surface is very complicated to get through traditional surface treatments [5]. Formation of unfavourable phases can take place to fabricated surface composite via liquid processing [6]. Furthermore, it is very difficult to get better mechanical and microstructural properties in surface composites. To avoid such complexities recently a new technique (friction stir processing) was developed. Friction stir processing (FSP) is a solid-state surface microstructural modification method developed from friction stir welding (FSW) technique is invented by The Welding Institute (TWI) of United Kingdom (UK) in 1991 [7, 8]. In FSP, rotating tool having designed shoulder and pin is plunged into material surface and traverse in the line of joint. Locally generated frictional heat plasticizes the material. This plastic deformation leads to microstructural changes in the deformation zone [9, 10, 11]. SMMCs composites are reinforced with variant reinforcement particles to obtain the individual properties of each together.

In this present research work, two nano reinforcement particles (Al₂O₃ and SiC) were used to fabricate the surface nanocomposites with varying volume percentages (2, 4 and 6 %) by applying single pass FSP.

2. MATERIALS AND METHODS

The base/matrix material used in this study was a commercial AA 6061-T6 Aluminum alloy, having the size of 4 mm thickness, 75 mm width and 150 mm length. Table 1 shows the matrix material chemical composition. Here, nano Al₂O₃ and SiC powders were selected as reinforcements particles with the average size of 40 – 50 nm.

Table 1. The chemical composition of as-received Al alloy

Element	Mg	Si	Cu	Zn	Ti	Mn	Cr	Al
wt.%	0.85	0.68	0.22	0.07	0.05	0.32	0.06	Bal.

A specially designed heat treated H13 tool steel tool (concave shoulder taper threaded cylindrical tool having a radius (r) = 3.5 mm) shown in Fig. 1 was used as FSP tool to fabricate the surface nanocomposites. All the dimensions shown in Fig. 1 are in millimeters (mm). To incorporate the reinforcement particles into the base material a square groove was made along the centre of the line of joint and tangent to the pin. The groove dimensions were changed as per the volume percentages taken as 2, 4 and 6 volume percentage respectively to produce surface nanocomposites. At the time of processing, there is a chance of escape of

---

∗ Corresponding author. Tel.: +91-9603-834664.
E-mail address: *askar86@yahoo.com* (N. Parumandla)

reinforcement particles from the groove; to avoid this kind of difficulty initially the groove was closed with FSP tool having no pin.
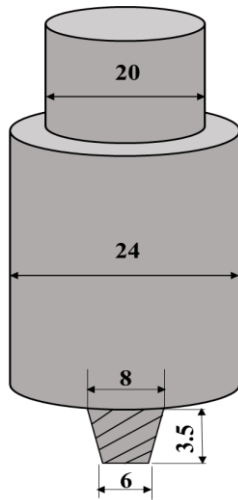
Fig. 1. Tool geometry of FSP tool

Table 2 shows, the process parameters used to fabricate the surface nanocomposites. With the help of ethanol, all the samples were cleaned to avoid the formation of oxides on the surface before FSP. Single pass FSP was applied to fabricate the surface nanocomposites.

Table 2. Process parameters and their values

Process parameters, units	Values
Tool rotational speed, rpm	1150
Tool traverse speed, mm/min	15
Axial force, kN	5
Tilt angle, degrees	2.5

All experiments were conducted on FSW machine having the three-ton capacity with the numerically controlled machine. By using wire cut electrical discharge machine, all the fabricated composites were cut as per ASTM standards (ASTM: E8/E8M-11 for tensile test and ASTM: G99-05 for wear) for studying the microstructural, mechanical and wear properties. Fig. 2 shows a schematic diagram of FSP.
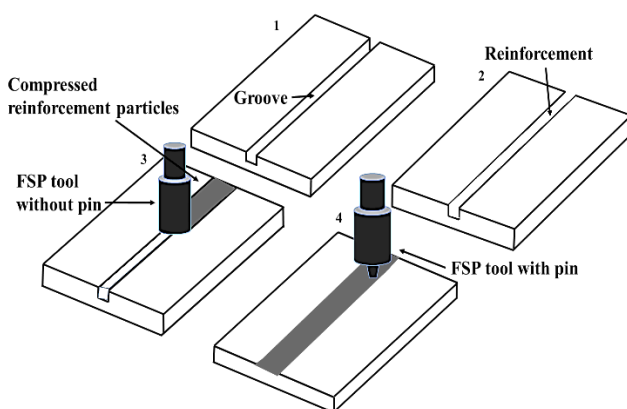
Fig. 2. Schematic operational diagram of FSP

Cross-sectioned composites were examined for microstructural studies by using an optical microscope (make: Madimage Technologies Pvt. Ltd; model: Prime – 100). Before that, samples were polished and etched with Keller's reagent (15 ml HNO_3, 6ml HCL, 4ml HF and 175 ml H_2O). For conducting microhardness test, Vickers microhardness tester (make: Chennai Metco Pvt. Ltd; model: ECONOMET VH-1) was employed. By applying 25 gm load with 15 seconds' dwell time, microhardness tests were conducted. Tensile tests were performed at a strain rate of 1×10^{-3} s^{-1} using an Instron tensile tester (make: HEICO; modle: HLC 693-30). The tensile fracture surfaces were examined by scanning electron microscope (SEM) (make: Tescan; model: Vega 3 LMU). Wear test (make: Magnum Engineers; model: TE-165-LE) was performed on pin – on disk machine.

3. RESULTS AND DISCUSSION

3.1. Macrostructure analysis

Fig. 3 shows the macroscopic appearance of the fabricated surface nanocomposite. From the visual observation, it is clear that all the surface nanocomposites were found to be defect free and the surface roughness of the fabricated composites was varied according to the increase in volume percentage of reinforcement and type of reinforcement is added. The semi-circular pattern was observed on the surface of the all fabricated composites.
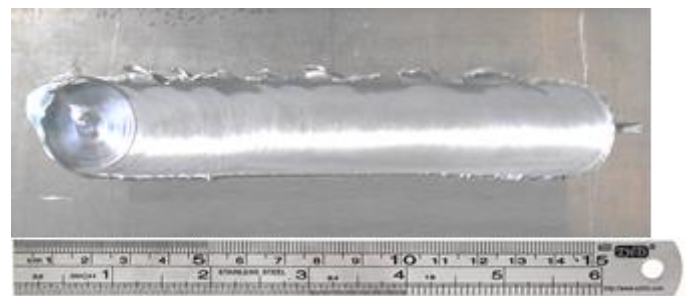
Fig. 3. Fabricated surface nanocomposite by FSP

3.2. Microstructure analysis

Microscopic examinations reveal that the process variables have a significant impact on the formation of surface nano composites. The nano Al_2O_3 and SiC particles were distributed in stir zone (SZ) concerning their volume percentages. The mixture (reinforcement and matrix material) of the plasticized material primarily yield from the advancing side (AS) and travels towards the retreating side (RS). On advancing of SZ, the material plasticization and forges towards the bottom of the pin. With the dynamic stirring action of the tool the packed reinforcement to mixes with the plasticized matrix to form the composite. A good mixture of the reinforcement particles with the matrix was observed in the fabricated composite.

During FSW/P, material flow plays a very important role during fabrication of good quality joints and it mainly depends on several factors like rotational speed of the tool, traverse speed, tool geometry and applied force, etc. The microstructures of Al/Al_2O_3 taken at various regions of fabricated surface nanocomposites are shown in Fig. 4. It is hard to obtain even distribution of reinforcement across SZ using single groove technique. During the fabrication process, different types of flow pattern took place and are shown in Fig. 4. From Fig. 4 a, it is seen that dragging material from the top surface of the material from the RS

into AS by tool shoulder. The concave geometry of the tool and large downward forces help the material to easily flow towards SZ from the upper layer of the material. Transitional zones (stir zone (SZ), thermomechanical heat affected zone (TMAZ) and Heat affect zone (HAZ)) are formed during the plasticization of material.
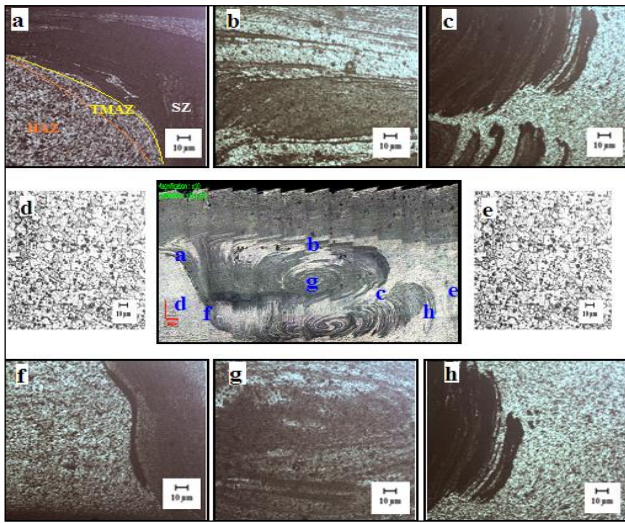
Fig. 4. Microstructure of material flow taken place during the fabrication of surface nanocomposites: a – transitional zone; b – shoulder driven region; c – material flow taken short turn during the process at RS; d – HAZ on AS; e – HAZ on RS; f – plasticized material flow forged by shoulder of the tool; g – centre of SZ; h – plasticized material flows travelling on AS from RS

It is hard to obtain even distribution of reinforcement across the SZ using single groove technique. During the fabrication process, different types of flow pattern took place and are shown in Fig. 4. From the Fig. 4 a, it is detected that dragging material from the top surface of the material from the RS into AS by tool shoulder. The concave geometry of the tool and large downward forces helps to the material to easily flow towards SZ from the upper layer of the material. Transitional zones (stir zone (SZ), thermomechanical heat affected zone (TMAZ) and Heat affect zone (HAZ)) were formed during the plasticization of material. A non-uniform mixture of the surface composite layer can be observed from Fig. 4 b. Tool rotational speed and transverse speed form dark and white coloured bands during the process. Fig. 4 c shows the flow of material on the RS. A quick return of material flow takes place during the process leading to the formation of onion ring like structures. A number of onion rings are formed at high tool rotational speeds with low traverse speeds. Fig. 4 d and e shows the HAZ regions formed during the process on AS and RS. It was seen that grain refinement occurred during the process. Large sizes of grains were observed at the HAZ region. A similar way of grain growth took place on the both sides of the processed region and it was also noticed that the size of the grain increased much like elongated grain while moving towards base metal (BM) region.

The geometry of the tool pin is incredibly significant in plasticization of material flow and its trend inside the deformation zone. At this point, the geometry of tool and pin is flexible to allow the rich mixture of reinforcement with matrix into the SZ as shown in Fig. 4 f. At the centre

of the SZ, formation of onion ring like structure can be seen in Fig. 4 g. Fig. 4 h shows the material is drawn towards the surface on the RS.

In FSW/P joining of materials by selection of improper tool geometry, process parameters and setting of tool location during the process, etc. From Fig. 5 it is shown that the surface composites were fabricated at constant process parameters like rotational speed and traverse speed of the tool with varying nano reinforcements. In this investigation at 1150 rpm tool rotational speed and 15 mm/min traverse speed defects were observed in Al/Al$_2$O$_3$ surface composite by the addition of 6 volume percentage of Al$_2$O$_3$ reinforcement. But in Al/SiC composite defects are found at 4 and 6 volume percentage of reinforcement composition. It means the defect formation does not only depend on the process parameters, tool geometry but also depends on reinforcement and its volume percentage.
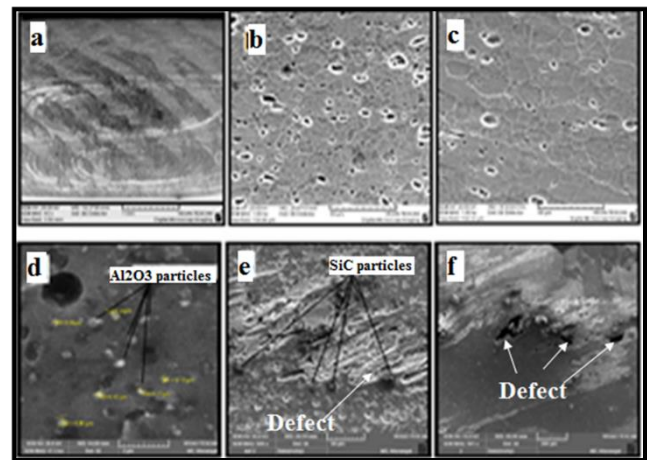
Fig. 5. SEM morphologies of fabricated composites: a – fabricated surface composite; b – refined grain structure of Al/Al$_2$O$_3$ composite; c – microstructure of Al/SiC composite; d – Al/Al$_2$O$_3$ composite; e – defect formed during process; f – voids are formed during Al/Al$_2$O$_3$ composite at 6 vol.%

Fig. 5 a shows that, the dispersion of reinforcement particles taken place after FSP. From the Fig. 5 b it is observed that the reinforcement particles were occupied with in the grains and at grain boundaries too. Most of the reinforcement particles were occupied on the boundaries of the grain shown in Fig. 5 c. From Fig. 5 d and e, the reinforcement of Al$_2$O$_3$ and SiC are well dispersed in the matrix. Nano particles size was increased more than doubled and led to agglomeration. Micro cracks are initiated at the boundaries of the pin region along the flow pattern of the material as shown in Fig. 5 e and f.

From Fig. 5 e and f it is observed that small micro cracks appeared at 4 volume percentage of SiC reinforcement and voids and tunnel like defect are observed at 6 volume percentage. Similar voids and tunnelling like defects are observed in Al/Al$_2$O$_3$ composite with 6 volume percentage composites shown in Fig. 5 f. Few researchers have studied the properties of Al/SiC composite [13]. They have produced a defect-free composite with single pass FSP through a smaller amount volume percentage of SiC reinforcement (approx. 1 volume percentage). Here the volume percentage was increased up to 4 for Al$_2$O$_3$ and 2 for SiC by applying single pass FSP.
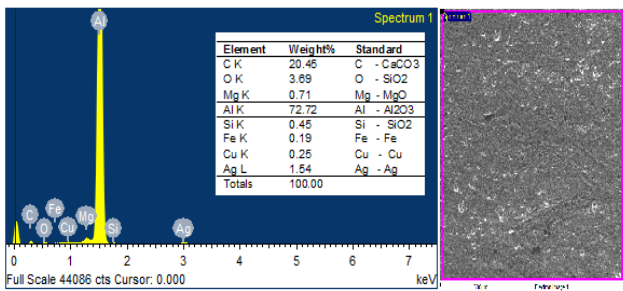
Fig. 6. EDS analysis of Al/Al$_2$O$_3$ surface nanocomposite
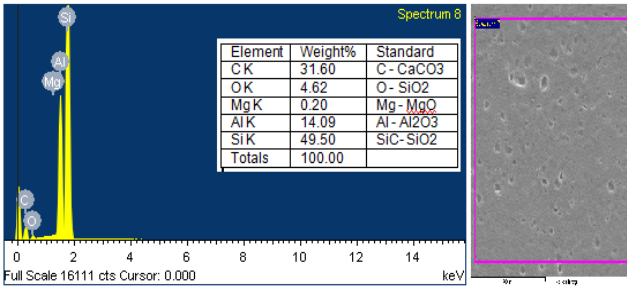
Fig. 7. EDS analysis of Al/SiC surface nanocomposite

The EDS analysis results of the fabricated Al/Al$_2$O$_3$ and Al/SiC are shown in Fig. 6 and Fig. 7. At the centre of the SZ of various ratios of composites were carried out to see the presence of Al$_2$O$_3$ and SiC reinforcements distribution. From Fig. 6 it is observed that the Al$_2$O$_3$ particles were well distributed into the matrix material and some other elements like Mg, Si, C, etc., were formed. Fig. 7 shows, the dispersion of the SiC particles into the matrix and other elements like Al, Mg and C also observed.

3.3. Microhardness

Fig. 8 shows the microhardness variations in the surface nanocomposite samples of Al/Al$_2$O$_3$ and Al/SiC.
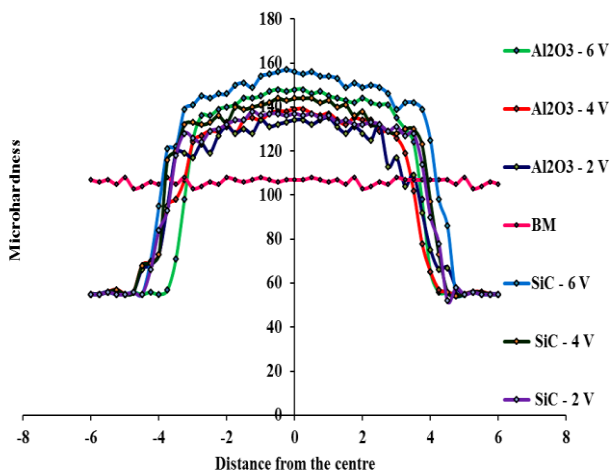
Fig. 8. Microhardness values of 2, 4 and 6 vol.% of Al/Al$_2$O$_3$ and Al/SiC composites fabricated at 1150 rpm with 15 mm/min

With the increase in volume percentage of the reinforcement, the microhardness of the samples was increased. Superior microhardness values were achieved because of microstructural enhancement due to FSP and strengthening mechanisms. Here the hardness of the surface composites increased based on strengthening mechanisms

(Hall-Petch relation and Orowan theory) [14]. The dispersion of the SiC and Al$_2$O$_3$ reinforcement particles and the grain refinement of the matrix through FSP increased hardness. A clear hardness divergence was observed between the SZ and the other transitional zones. The temperatures distribution during the FSP was may be the reason for hardness dissimilarity in transitional zones. The presence of reinforcement particles Al$_2$O$_3$ and SiC in the SZ, aging and ultrafine microstructure improved the microhardness in SZ [15]. Mainly in Aluminum metal matrix composites (AMMCs) increased hardness was achieved basically due to nature of the reinforcement particles added and the uneven thermal expansion coefficient of reinforcement and matrix phases caused by dislocation [16].

A clear hardness disparity was noticed between the Al/Al$_2$O$_3$ and Al/SiC composites. Higher hardness values were shown in Al/SiC composites than Al/Al$_2$O$_3$. At each level of volume percentage, Al/SiC composites dominated Al/Al$_2$O$_3$ composites. It may be due to the presence of hard ceramic and carbide particles of reinforcement. However, the hardness values attained by adding nano reinforcement particles are superior as compared to the base material shown in Table 3.

Table 3. Microhardness values of surface nanocomposites

Sample	Microhardness, Hv*
2v – Al$_2$O$_3$	132
4v – Al$_2$O$_3$	139
6v – Al$_2$O$_3$	148
2v – SiC	137
4v – SiC	144
6v – SiC	156
Base material (BM)	107
*Avg. Values of three samples.	

3.4. Tensile test and fractography

The extracted tensile properties (Young's modulus (YS), ultimate tensile strength (UTS) and elongation (El)) of fabricated surface nanocomposites are shown in Table 4.

Table 4. Tensile values of surface nanocomposites

Sample	Ultimate tensile strength, MPa*	Yield strength, MPa*	Eelongation, %*
BM	295	271	12
2v – Al$_2$O$_3$	172.7	142.6	8.4
4v – Al$_2$O$_3$	184.5	158.5	6.9
6v – Al$_2$O$_3$	129.2	105.7	4.6
2v – SiC	179.4	153.7	7.1
4v – SiC	131.6	114.4	4.8
6v – SiC	110.4	94.3	3.2
*Avg. values of 3 samples.			

In summary, the tensile properties of the composites decreased with an increase in volume percentage of the reinforcement into the matrix. Many factors determine the tensile strength of AMMCs. These are (i) presence of defects in the deformation zone, (ii) improper mixing of reinforcement and base material, (iii) HAZ grain size and (iv) over aging and dissolution of precipitation [17]. The tensile test was performed at defect free condition (1150 rpm and 15 mm/min) obtained by the tool having

shoulder diameter of 24 mm and compared with the result of 6061 T6 Al alloy properties. All the composites were tested from tensile to know the UTS, YS and % EL. Each sample was tested three times, and the average value of them is presented in Table 4.
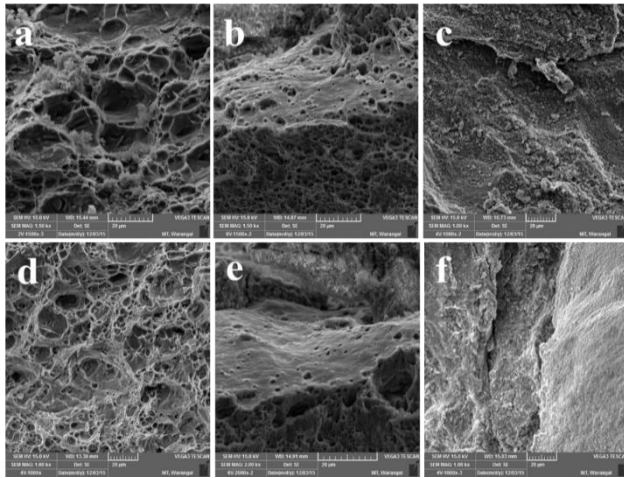
Fig. 9. SEM fractography's: $a-2v-Al/Al_2O_3$; $b-4v-Al/Al_2O_3$; $c-6v-Al/Al_2O_3$; $d-2v-Al/SiC$; $e-4v-Al/$ SiC; $f-6v-Al/$ SiC

Fig. 9 shows the SEM fractography of the fabricated surface composite of Al/Al_2O_3 and Al/SiC by varying 2, 4 and 6 volume percentage of reinforcement. A ductile failure was observed from the sample of Al/Al_2O_3 and Al/SiC. The nano reinforcement particles are pulled away from the matrix by leaving the impressions like dimples on the matrix. The dislocation density of the composites was increased which leads to a reduction of elongation. Fractured surface of the composites shows larger dimples with reduced ductility. Also, the existence of ceramic particles becomes impalpable the moment plasticized base material increased its brittleness to a certain extent. The failures were ductile type failure since the characteristic fine dimples were observed. Cup and cone like failure can also be observed.

3.4. Wear characterization

To study the influence of nano Al_2O_3 and SiC particles on the wear resistance of fabricated FSPed composite were investigated. The wear rate and coefficient of friction were plotted against the Al_2O_3 and SiC relative ratios of volume percentages (2, 4 and 6) and sliding distance respectively. The relation between the coefficient of friction and sliding distance while varying the volume percentage of the reinforcement of the samples were shown in Fig. 10 and Fig. 11. From Fig. 10 it is observed that the coefficient of friction between the fabricated surface nanocomposites (Al/Al_2O_3 at 2, 4 and 6 volume percentages) and the disk (steel disk) was almost same during the tests. The average coefficient of friction values exhibited general tendency to decrease or increase with the relative content of reinforcement into the matrix material. The coefficient of friction between the disk and the sample surface was not affected by the volume percentage of the reinforcement, but the type of reinforcement influences it.

Fig. 11 shows the coefficient of friction values obtained during the wear test of Al/SiC surface nanocomposites. The initial increase in the coefficient of friction may be due to the increase in the frictional force needed to overcome the highly adhesive contact between the ball and the tested surface. The average coefficient of friction Al/Al_2O_3 is 0.5, and Al/SiC is 0.24 as shown in Fig. 10 and Fig. 11. It means the Al_2O_3 powder had a higher frictional coefficient than that of SiC when they were tested under the same conditions. Therefore, it may be expected that the composites that contained higher ratios of SiC particles will have lower friction coefficients.
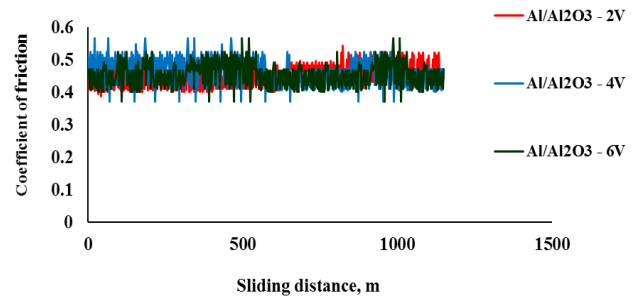
Fig. 10. The friction coefficient of the Al/Al_2O_3 surface composite as a function of sliding distances at an applied load of 20 N
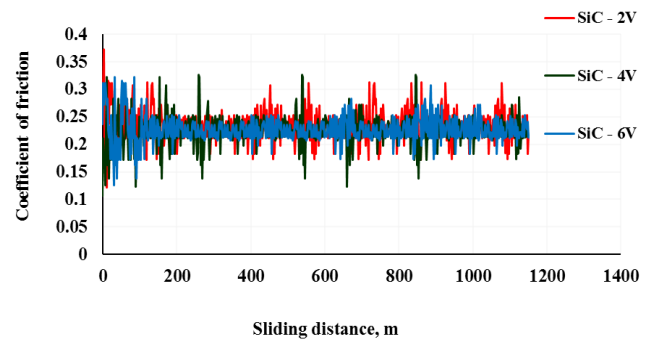
Fig. 11. The friction coefficient of the Al/SiC surface composite as a function of sliding distances at an applied load of 20 N

The effect of Al_2O_3 and SiC nano reinforcement on wear rate were compared with the as received base material was shown from the Fig. 12 and Fig. 13. With the increase in volume percentage of the reinforcement of Al_2O_3 and SiC, the wear resistance was decreased and shown less wear rate at a higher volume percentage of surface composites. When the composites (Al/Al_2O_3 and Al/SiC) were tested under the same conditions, Al/SiC composites were shown better results (lower wear rate) than Al/Al_2O_3 composites.
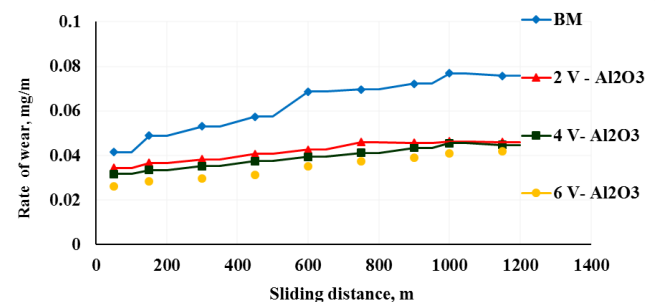
Fig. 12. Variation in the rate of wear with sliding distance for Al/Al_2O_3 surface nanocomposites

342

During the initial stage of wear test, the wear rate was increased with sliding distance, but after a certain distance, the removal rate of material from the sample decreases with increase in sliding distance. Fig. 12 and Fig. 13 show the addition of Al_2O_3 and SiC reinforcement to matrix material (aluminium) was advantageous in reducing the wear rate.
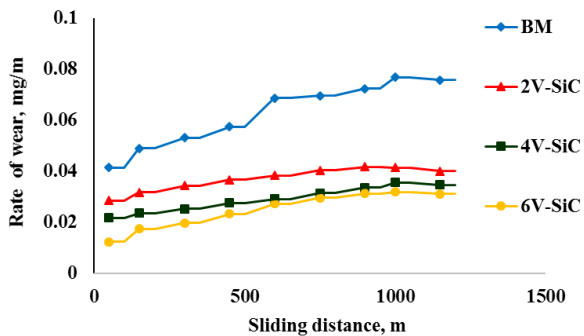
Fig. 13. Variation in the rate of wear with sliding distance for Al/SiC surface nanocomposites
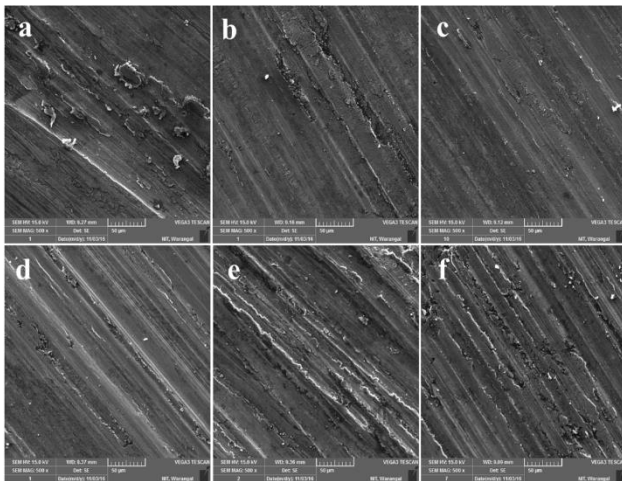
Fig. 14. SEM micrographs of worn surfaces of fabricated surface nanocomposites: $a-2V-Al/Al_2O_3$; $b-4V-Al/Al_2O_3$; $c-6V-Al/Al_2O_3$; $d-2V-Al/SiC$; $e-4V-Al/SiC$; $f-6V-Al/SiC$

Fig. 14 show the wear morphology of Al/Al_2O_3 and Al/SiC surface nano composites tested at same conditions of load and distance. The effect of the coefficient of friction can be observed through the Fig. 14. A clear view of grooves can be observed on the surface of the nano composite of Al/SiC sample than Al/Al_2O_3 sample.

The addition of the reinforcement particles (Al_2O_3 and SiC) into the matrix material leads to lower wear resistance. The surface nanocomposites of Al/Al_2O_3 with varying volume percentage (2, 4 and 6) are shown in Fig. 14 a, b, and c. Here the presence of Al_2O_3 particle leads to solid lubricant between the steel disk and surface of the composite [18, 19]. The Al_2O_3 particles pulled out from the surface of the composite and formed like a layer on the surface of the worn composite surfaces. This layer formation reduces the coefficient of friction between the surface of the composite and disk which reduces the rate of wear and if can be observed in Fig. 14 a, b, and c. On the other hand, the test the hard-ceramic particles restrict the material removal rate from the components [20 – 22]. From Fig. 14 d, e, and f it can be observed that the Al/SiC composites show less wear

rate than compared with Fig. 14 a, b, and c. Here hard SiC particles are acted as load bearing components and reduced material removal rate. With the increase in volume percentage of reinforcement, the material removal rate is decreased as shown in Fig. 14.

4. CONCLUSIONS

In the present work, the fabrication of Al/Al_2O_3 and Al/SiC surface nanocomposites were fabricated with varying volume percentage of reinforcements (2, 4 and 6) by the FSP. The microstructure, microhardness, mechanical and wear behaviour were examined. The obtained outcomes were summarised as follows:

1. Successfully Al/Al_2O_3 surface nanocomposites were fabricated up to 4 volume percent of reinforcement, and Al/SiC were fabricated at 2 volume percentage only with applying single pass FSP.
2. The addition of the nano reinforcement particles (Al_2O_3 and SiC) was more effectively reduced the grain size at the SZ of the composites because of pinning effect by the reinforcement particles restricted the grain growth of Al matrix grains (dynamically recrystallized grains).
3. The microhardness of the Al/Al_2O_3 and Al/SiC composites were increased significantly with increasing volume percentage of reinforcement particles. Higher microhardness values were obtained at 6 volume percentage of Al/SiC surface nanocomposite (i.e., 156 Hv at SZ).
4. Good tensile strength results were obtained at 4 volume percentage of Al/Al_2O_3 surface nanocomposite (i.e., 184.5 MPa).
5. With the addition of reinforcement particles, wear resistance of the surface nanocomposites was increased significantly. At 6 volume percentage of Al/Al_2O_3 and Al/SiC surface nanocomposites exhibits superior wear resistance properties on an average of (i.e., 0.0344 mg/m and 0.0248 mg/m).

REFERENCES

1. **Smagorinski, M., Tsantrizos, P., Grenier, S., Entezarian, M., Ajersch, F.** The Thermal Plasma Near-Net-Shape Spray Forming of Al Composites *The Journal of the Minerals, Metals & Materials Society* 48 (6) 1996: pp. 56 – 59.
https://doi.org/10.1007/BF03222970

2. **Vijaya Ramnath, B., Elanchezhian, C., Annamalai, R.M., Aravind, S., Sri Ananda Atreya, T., Vignesh, V., Subramanian, C.** Aluminium Metal Matrix Composites – A Review *Reviews on Advanced Materials Science* 38 (1) 2014: pp. 55 – 60.

3. **Mishra, R.S., Ma, Z.Y., Charit, I.** Friction Stir Processing: A Novel Technique for Fabrication of Surface Composite *Materials Science and Engineering A* 341 2014: pp. 307 – 310.
https://doi.org/10.1007/978-3-319-07043-8_9

4. **Cavalierea, P., Squillace, A.** High Temperature Deformation of Friction Stir Processed 7075 Aluminium Alloy *Materials Characterization* 55 2005: pp. 136 – 142.
https://doi.org/10.1016/j.matchar.2005.04.007

5. **Mishra, R.S., Ma, Z.Y.** Friction Stir Welding and Processing *Materials Science and Engineering R* 50 2005: pp. 1 – 78.
https://doi.org/10.1016/j.mser.2005.07.001

6. **Mahmoud, E.R.I., Takahashi, M., Shibayanagi, T., Ikeuchi, K.** Wear Characteristics of Surface-Hybrid-Mmcs Layer Fabricated on Aluminium Plate by Friction Stir Processing *Wear* 268 2010: pp. 1111 – 1121.
https://doi.org/10.1016/j.wear.2010.01.005

7. **Budinski, K.G.** Surface Engineering for Wear Resistance Prentice-Hall, NewJer-sey 1988: pp. 1 – 348.

8. **Shafiei-Zarghani, A., Kashani-Bozorg, S.F., Zarei-Hanzaki, A.** Microstructures and Mechanical Properties of Al/Al_2O_3 Surface Nano-Composite Layer Produced by Friction Stir Processing *Materials Science and Engineering A* 500 2009: pp. 84 – 91.
https://doi.org/10.1016/j.msea.2008.09.064

9. **Mishra, R.S., Mahoney, M.W., McFadden, S.X., Mara, N.A., Mukherjee, A.K.** High Strain Rate Superplasticity in a Friction Stir Processed 7075 Al Alloy *Scripta Materialia* 42 (2) 2000: pp. 163 – 168.
https://doi.org/10.1016/S1359-6462(99)00329-2

10. **Thomas, W.M., Nicholas, E.D., Needham, J.C., Murch, M.G., Templesmith, P., Dawes, C.J.G.B.** Patent Application No, 9125978.8, December 1991.

11. **Mishra, R.S., Mukherjee, A.K.** Processing of High Hardness-High Toughness Alumina Matrix Nanocomposites *Materials Science and Engineering A* 301 2001: pp. 97 – 101.
https://doi.org/10.1016/S0921-5093(00)01381-2

12. **Colligan, K.** Material Flow Behavior During Friction Stir Welding of Aluminum *Welding Journal* 65 1999: pp. 229 – 233.

13. **Seidel, T.U., Reynolds, A.P.** Visualization of the Material Flow in AA2195 Friction-Stir Welds Using a Marker Insert Technique *Metallurgical and Materials Transactions A* 32 2001: pp. 2879 – 2887.
https://doi.org/10.1007/s11661-001-1038-1

14. **Salehi, M., Saadatmand, M., Aghazadeh Mohandesi, J.** Optimization of Process Parameters for Producing AA6061/Sic Nanocomposites by Friction Stir Processing *Transactions of Nonferrous Metals Society of China* 22 2012: pp. 1055 – 1063.
https://doi.org/10.1016/S1003-6326(11)61283-1

15. **Dawood, H.I., Mohammed, K.S., Rahmat, A., Uday, M.B.** Effect of Small Tool Pin Pro-Files on Microstructures and Mechanical Properties of 6061 Aluminum Alloy by Friction Stir Welding *Transactions of Nonferrous Metals Society of China* 25 2015: pp. 2856 – 2865.
https://doi.org/10.1016/S1003-6326(15)63911-5

16. **Mahmoud, E.R.I., Takahashib, M., Shibayanagib, T., Ikeuchi, K.** Wear Characteristics of Surface-Hybrid-Mmcs Layer Fabricated on Aluminum Plate by Friction Stir Processing *Wear* 268 2010: pp. 1111 – 1121.
https://doi.org/10.1016/j.wear.2010.01.005

17. **Palanivel, R., Koshy Mathews, P., Murugan, N., Dinaharan, I.** Effect of Tool Rotational Speed and Pin Profile on Microstructure and Tensile Strength of Dissimilar Friction Stir Welded AA5083-H111 and AA6351-T6 Aluminum Alloys *Materials and Design* 40 2012: pp. 7 – 16.
https://doi.org/10.1016/j.matdes.2012.03.027

18. **Gui, M., Kang, S.B.** Aluminum Hybrid Composite Coatings Containing Sic and Graphite Particles by Plasma Spraying *Materials Letters* 51 (5) 2001: pp. 396 – 401.
https://doi.org/10.1016/S0167-577X(01)00327-5

19. **Tjong, S.C., Lau, K.C., Wu, S.Q.** Wear of Al-based hybrid composites containing BN and SiC Particulates *Metallurgy and Materials Transactions A* 30 199: pp. 2551 – 2555.
https://doi.org/10.1007/s11661-999-0265-8

20. **Gurcan, A.B., Baker, T.N.** Wear Behaviour of AA6061 Aluminium Alloy and its Composites *Wear* 188 1995: pp. 185 – 191.
https://doi.org/10.1016/0043-1648(95)06639-X

21. **Saravanan, R.A., Lee, J., Kang, S.** Dry Sliding Wear Behavior of A356-15 Pet Sic Composites Under Controlled Atmospheric Conditions *Metallurgy and Materials Transactions A* 30 1999: pp. 2523 – 2538.
https://doi.org/10.1007/s11661-999-0261-z

22. **Lee, J.M., Kanga, S.B., Han, J.** Dry Sliding Wear of MAO-Coated A356/20 Vol.% Sicp Composites in the Temperature Range 25 – 180 °C *Wear* 264 2008: pp. 75 – 85.
https://doi.org/10.1016/j.wear.2007.01.044